Supporting information

Cobalt pyrophosphate ($Co_2P_2O_7$) derived from an Open-Framework Cobalt Phosphite: A Durable Electroactive Material for Electrochemical Energy Conversion and Storage Application

Abhisek Padhy, [a, b, c] *Aneeya K. Samantara,* [a, b, c] *J. N. Behera* [a, b, c*]

[a] National Institute of Science Education and Research (NISER), Khordha 752050, Odisha, India

[b] Homi Bhabha National Institute, (HBNI), Mumbai, India

[c] Centre for Interdisciplinary Sciences (CIS), NISER, Jatni, Odisha, India 752050.

*Email: jnbehera@niser.ac.in

➢ Calculation of electrochemical accessible surface area

At first, the double layer capacitance (C_{dl}) was calculated by plotting the cathodic and anodic peak currents (i) against the sweep rate (ϑ) as per the equation 1. Thereafter the ECSA and roughness factor (R_f) were determined accordingly (equation 2 and 3). [1,2]

$$C_{dl} = \frac{i}{\vartheta} \quad (1)$$

$$ECSA = \frac{C_{dl}}{C_s} \quad (2)$$

$$R_f = \frac{ECSA}{G_s} \quad (3)$$

Here, C_s is the standard specific capacitance of an atomically smooth metal oxide surface in alkaline electrolytic condition and its value is 40 μF/cm^2 and the G_s (geometrical surface area) of the electrode is 1 cm^2.

➢ Calculation of specific capacitance, energy and power

The specific capacitance (C_{sp}), energy (E_D) and power (P_D) were calculated from the CVs recorded at different sweep rates as per the following equations, [3,4]

$$C_{sp} = \frac{\int_{V_a}^{V_c} I(V)dV}{m\vartheta(V_c - V_a)} \quad (4)$$

$$E_D = \frac{C_{sp}(\Delta V)^2}{2} \quad (5)$$

$$P_D = \frac{C_{sp}(\Delta V)\vartheta}{2} \quad (6)$$

Here, $\int_{V_a}^{V_c} I(V)dV$, m, ϑ, $(V_c - V_a)$ and ΔV are the integrated surface area under the CV curve, mass of the electrode material loaded on the electrode surface, sweep rate and potential window respectively.

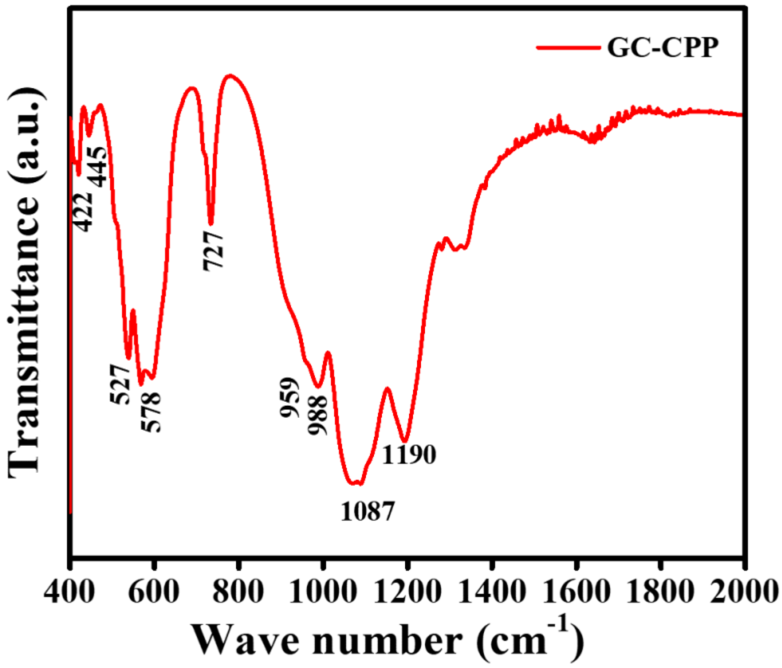

Fig. S1 FTIR spectrum of GC-CPP

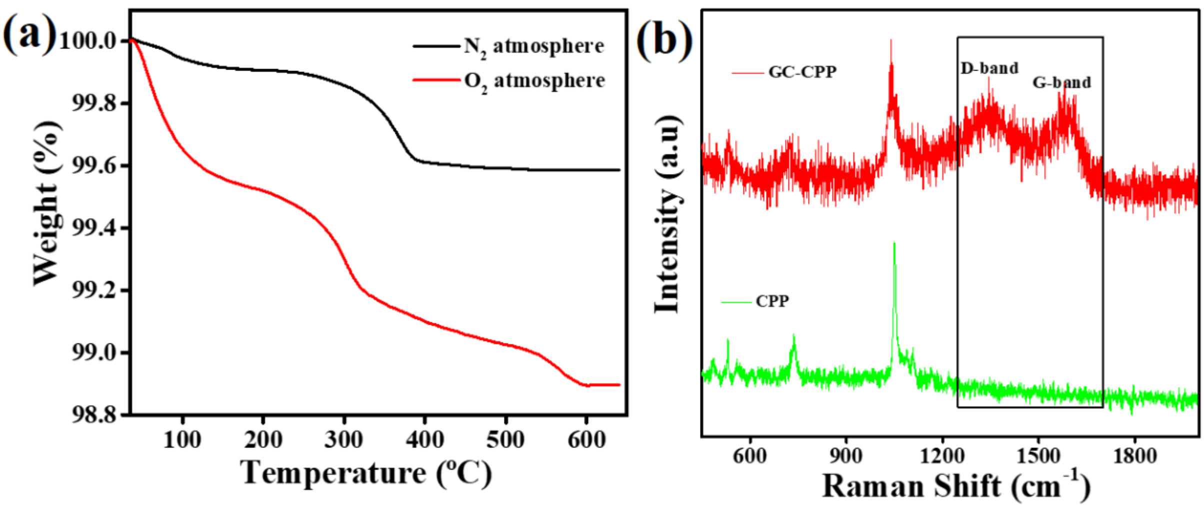

Fig. S2 (a) Thermo gravimetric analysis of GC-CPP in N_2 and air and (b) the corresponding Raman spectra.

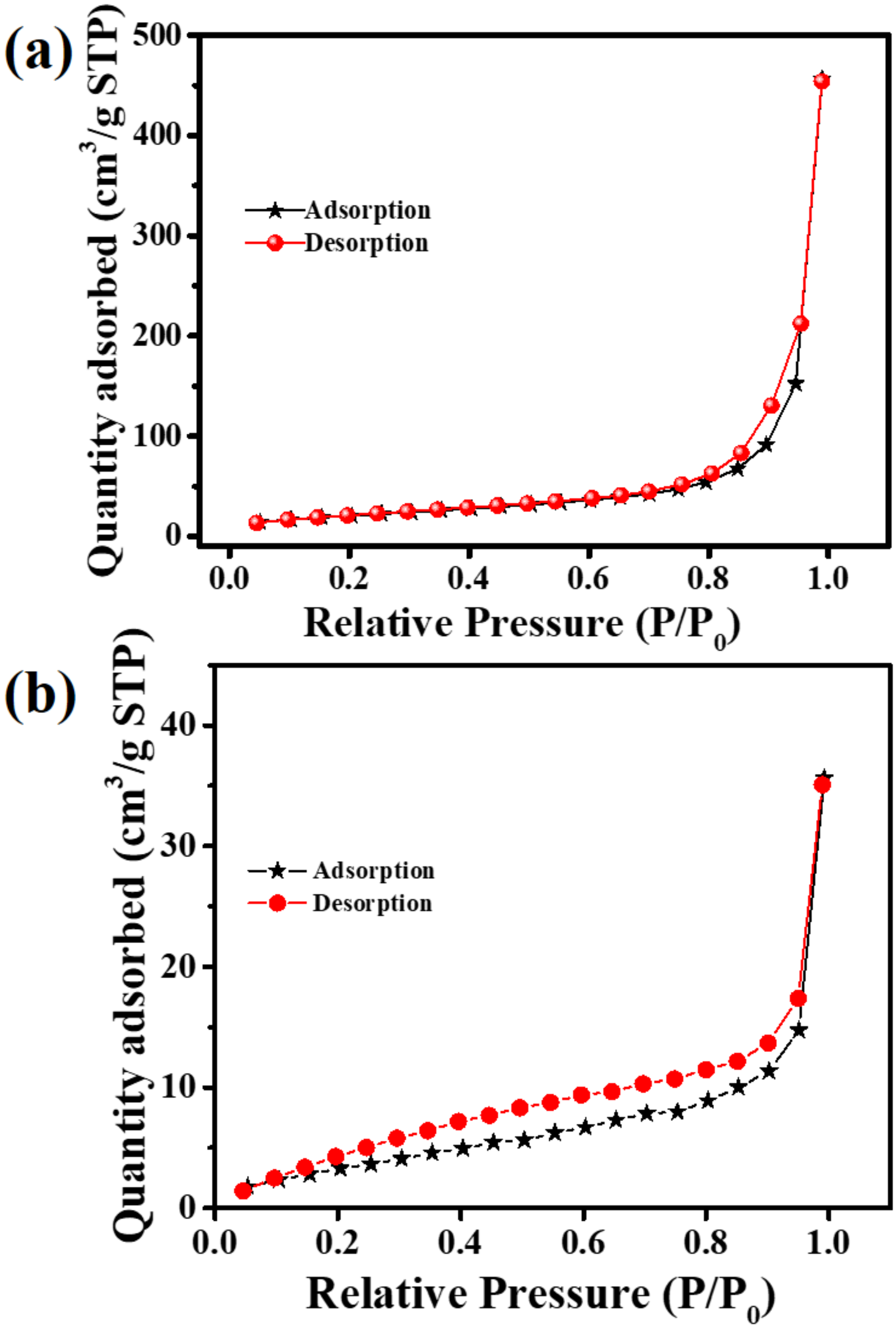

Fig. S3 BET adsorption/desorption isotherms for (a) CoHPO–CJ2 and (b) GC-CPP.

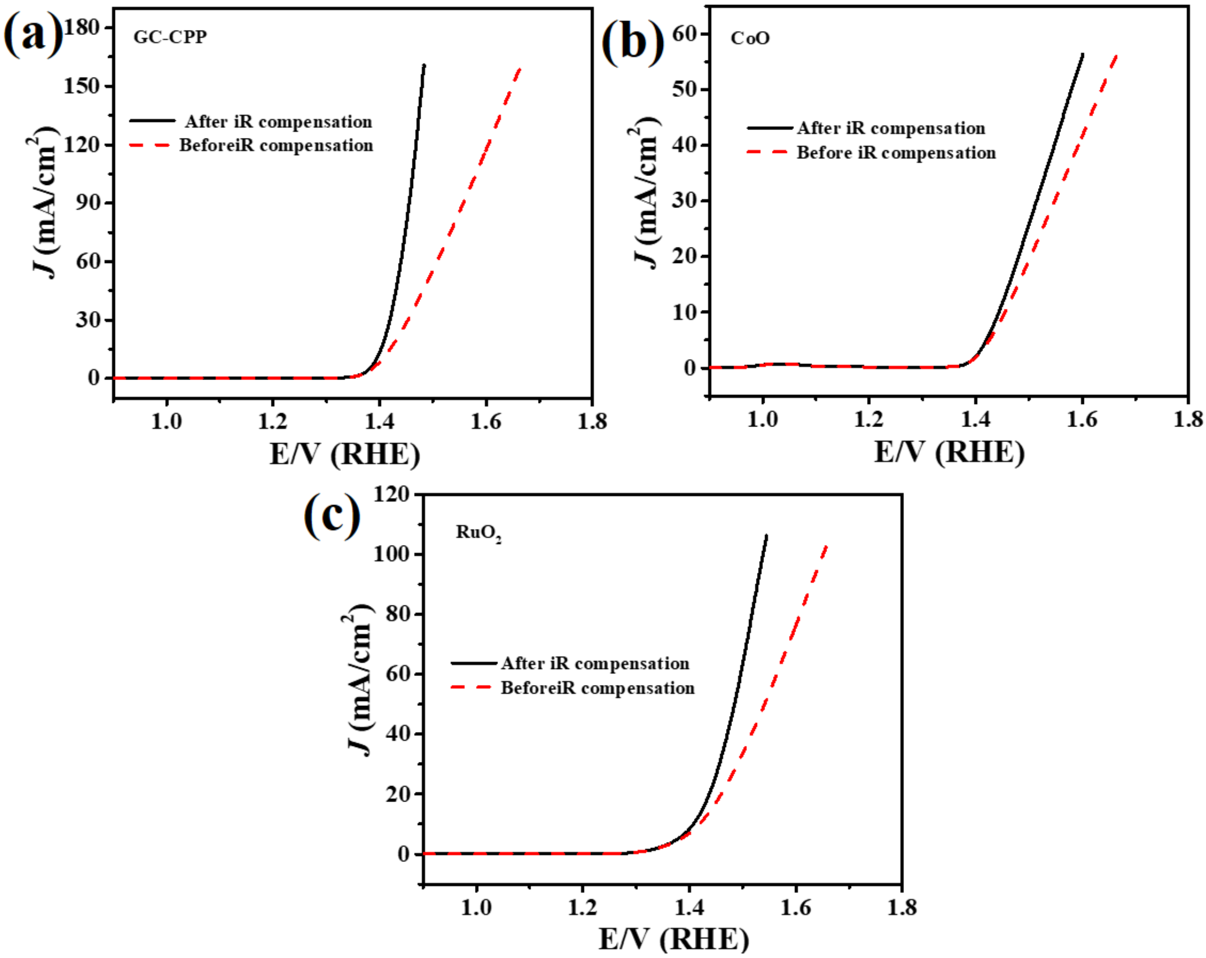

Fig. S4 Linear sweep voltammograms of GC-CPP, CoO and RuO_2 before and after iR-compensation.

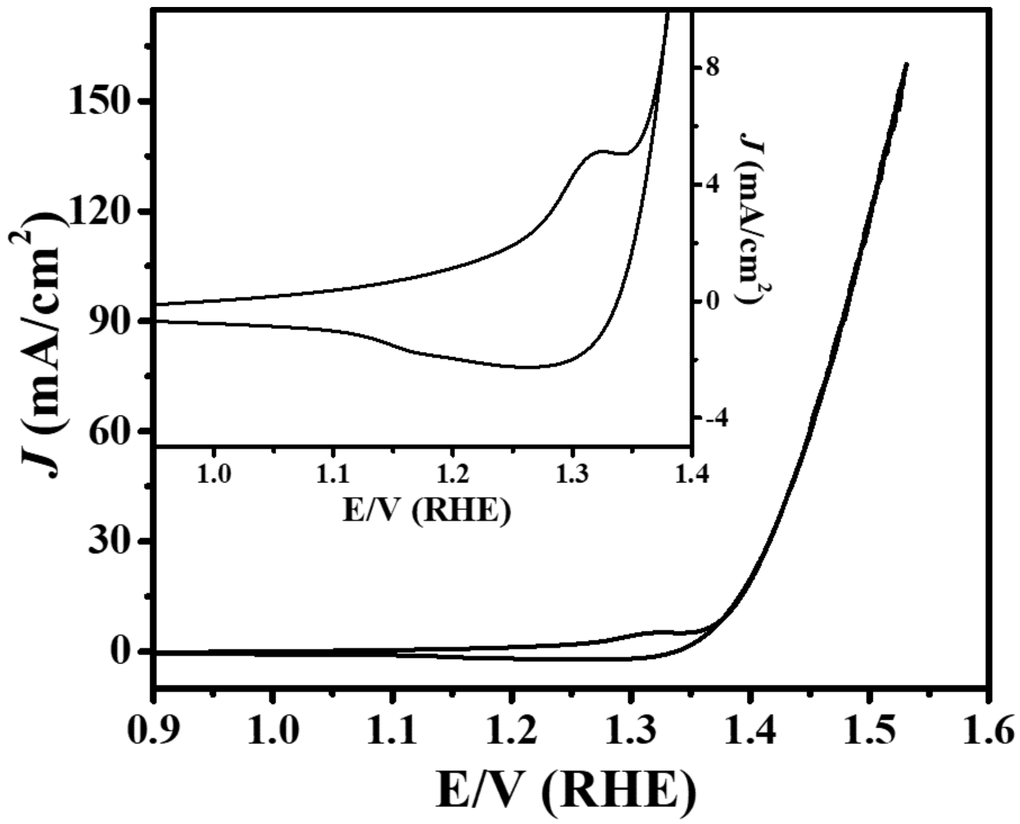

Fig. S5 Cyclic voltammogram of GC-CPP at 5 mV/s in 1M KOH electrolyte.

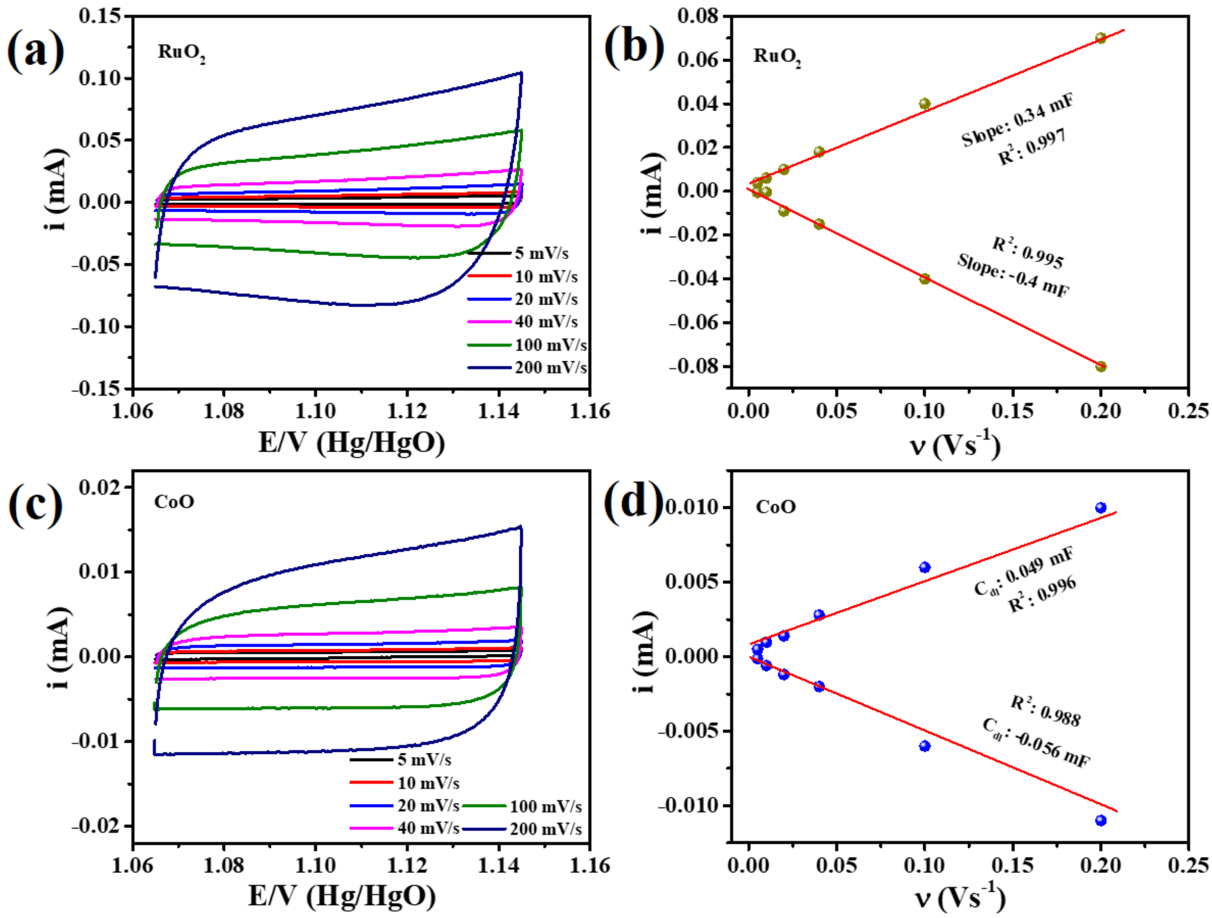

Fig. S6 (a, c) cyclic voltammograms at different sweep rate in non-Faradic potential window and (b, d) plot of cathodic and anodic current against sweep rate.

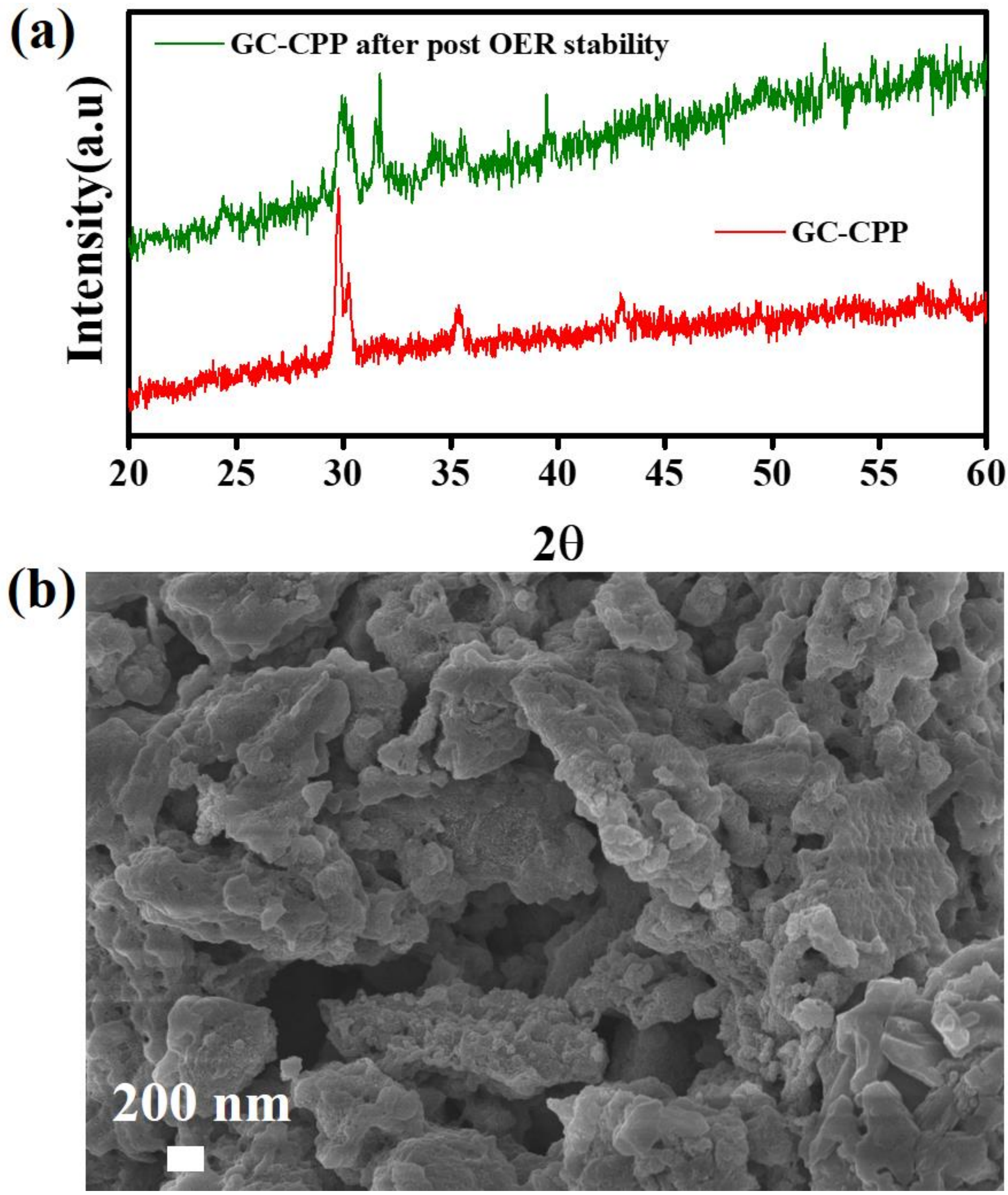

Fig. S7 (a) PXRD and (b) FESEM of post OER GC-CPP sample

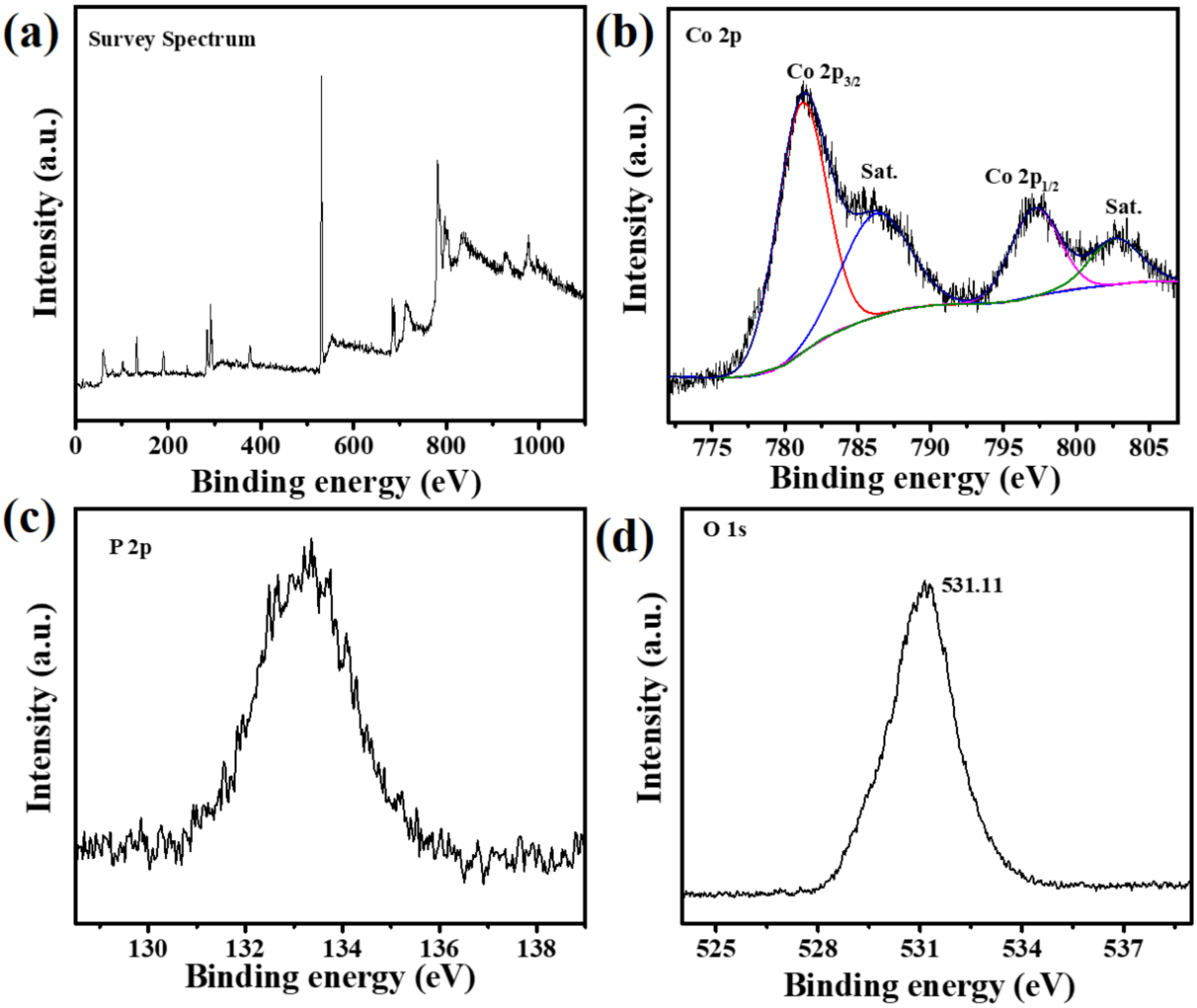

Fig. S8 (a) survey and high-resolution X-ray photoelectron spectrum of (b) Co 2p, (c) P 2p, (d) O 1s and (e) C 1s of GC-CPP after OER stability measurement.

Sample	Loading (mg/cm^2)	Tafel slope (mV/dec)	Overpotential (V) @ 10 mA/cm^2	Electrolyte (M)	Electrode	TOF (s^{-1})	ECSA (cm^2)	R_f	Ref.
Ultrafine CoP-CNT	0.28	50	0.330	0.1 (NaOH)	GCE	0.0287	--	--	5
CoP NRs/C	0.71	71	0.32	1 M KOH	GCRDE	--	--	--	6
CoP NPs/C	0.71	99	0.34	1		--	--	--	
CoMnP	0.28	61	0.33	1	GCRDE	--	--	--	7
Co_2P	0.28	128	0.37	1		--	--	--	
Co_2P (Nanoneedles)	0.2	50	0.31	1		--	--	--	8
$Co_3(PO_4)_3$@N–C	0.2	62	0.317	1	GCRDE	--	--	--	9
CoFePi	0.25	33	0.315	0.1	GCRDE	--	107	1514	10
CoFePi	0.25	31	0.277	1		--	--	--	
CoPi	0.25	61	0.388	0.1			61	864	
FePi + CoPi	0.25	51	0.355	0.1		--	--	--	
CoNiPi	0.25	87	0.402	0.1		--	--	--	
CoCePi	0.25	75	0.374	0.1		--	--	--	
CoFeNiPi	0.25	51	0.309	0.1		--	--	--	
NCoM-SS-Ar	0.14	76	0.340	1	GCRDE	--	--	--	11
Mesoporous CoPi-1	0.2	58.7	0.380	1	GCRDE	0.018	--	--	12
Hollow $Co_3(PO_4)_2$	0.12	84	N.A.	1	GCRDE	--	--	--	13
$Co_3(OH)_2(HPO_4)_2$/NF	2	69	0.240	1	NF	4.38×10^{-3}	2.52	--	14
$Co_2P_2O_7$	0.5	54.1	0.359	1	GCE	0.058	231.5	1837.3	15
$Na_2Co_{0.75}Fe_{0.25}P_2O_7$/C NPs	-	47	0.300	0.1	GCE	--	--	--	16
$Co_2(P_2O_7)$	0.5	41	0.165	1	Stainless steel mesh	7.95	13.52	13.52	Present work

Table S1 OER performance comparison of GC-CPP with reported materials. GCE: glassy carbon electrode, GCRDE: glassy carbon rotating disk electrode, NF: nickel foam

Table S2 Charge storage performance comparison of GC-CPP with reported materials

Materials	Specific Capacitance (F/g)	Potential window (V)	Current density (A/g)	Energy density (Wh/kg)	Power density (W/kg)	Reference
$Co_2P_2O_7$ + AB + PVDF on NF	367 in 3M KOH	0.40	0.625	8.16	125	17
$Co_{0.2}Ni_{0.8}$ Pyrophosphate	1259 in 3M KOH	0.55	1.5	42.4 (Device)	800	18
$Co_{0.6}Ni_{1.6}P_2O_7$/NG+ AB + PTFE on NF	1473	0.50	1.0	34.9 (Device)	800	19
$Co_2P_2O_7$ + Super P carbon + PVDF with redox additive in the electrolyte on Carbon paper.	580	0.7	1.0	-	-	20
$CoHPO_4.3H_2O$ + AB + PTFE on NF	413	0.45	1.5	-	-	21
$Co_3(PO_4)_2$ grown on NF	12,285 in 1M KOH @ 5mV/s	0.7	-	26.66 (Device)	750	22
Nickel–Cobalt Phosphate (Ni/Co = 4:5) on NF	1132.5 in 3M KOH	0.4	1.0	-	-	23
Co3(PO4)2.8H2O on NF	350 in 3M KOH	0.4	1.0	-	-	24
$Ni_3P_2O_8$-$Co_3P_2O_8$ (Ni/Co = 8:2)	1974 in 6M KOH	0.4	0.5	33.4 (device)	399	25
$Co_2(P_2O_7)$	900 in 5 M KOH at 1 mV/s 500 F/g	0.45	- 1.5	31.25	21 kW/kg	Present work

References:

1. M. K. Sahoo, A. K. Samantara and J. N. Behera, *Inorg. Chem.*, 2020, **59**, 12252–12262.
2. C. C. L. McCrory, S. Jung, J. C. Peters and T. F. Jaramillo, *J. Am. Chem. Soc.*, 2013, **135**, 16977–16987.
3. R. Ding, L. Qi and H. Wang, *J. Solid State Electrochem.*, 2012, **16**, 3621–3633.
4. S. Ratha, A. K. Samantara, K. K. Singha, A. S. Gangan, B. Chakraborty, B. K. Jena and C. S. Rout, *ACS Appl. Mater. Interfaces*, 2017, **9**, 9640–9653.
5. K. H. Cho, D. H. Shin, J. Oh, J. H. An, J. S. Lee and J. Jang, *ACS Appl. Mater. Interfaces*, 2018, **10**, 28412–28419.
6. J. Chang, Y. Xiao, M. Xiao, J. Ge, C. Liu and W. Xing, *ACS Catal.*, 2015, **5**, 6874–6878.
7. D. Li, H. Baydoun, C. N. Verani and S. L. Brock, *J. Am. Chem. Soc.*, 2016, **138**, 4006–4009.
8. A. Dutta, A. K. Samantara, S. K. Dutta, B. K. Jena and N. Pradhan, *ACS Energy Lett.*, 2016, **1**, 169–174.
9. C. Z. Yuan, Y. F. Jiang, Z. Wang, X. Xie, Z. K. Yang, A. Bin Yousaf and A. W. Xu, *J. Mater. Chem. A*, 2016, **4**, 8155–8160.
10. Y. Zhou and H. C. Zeng, *Small*, 2018, **14**, 1704403.
11. R. Gond, D. K. Singh, M. Eswaramoorthy and P. Barpanda, *Angew. Chemie*, 2019, **31**, 8418-8423.
12. M. Pramanik, C. Li, M. Imura, V. Malgras, Y. M. Kang and Y. Yamauchi, *Small*, 2016, **12**, 1709–1715.
13. J. Zhang, Y. Yang, Z. Zhang, X. Xu and X. Wang, *J. Mater. Chem. A*, 2014, **2**, 20182–20188.
14. P. W. Menezes, C. Panda, C. Walter, M. Schwarze and M. Driess, *Adv. Funct. Mater.*, 2019, **29**, 1808632.
15. H. Du, W. Ai, Z. L. Zhao, Y. Chen, X. Xu, C. Zou, L. Wu, L. Su, K. Nan, T. Yu and C. M. Li, *Small*, 2018, **14**, 1801068.
16. H. J. Song, H. Yoon, B. Ju, D. Y. Lee and D. W. Kim, *ACS Catal.*, 2020, **10**, 702–709.
17. H. Pang, Z. Yan, Y. Ma, G. Li, J. Chen, J. Zhang, W. Du and S. Li, *J. Solid State Electrochem.*, 2013, **17**, 1383–1391.
18. C. Chen, N. Zhang, Y. He, B. Liang, R. Ma and X. Liu, *ACS Appl. Mater. Interfaces*, 2016, **8**, 23114–23121.

19 P. Sun, Z. Li, L. Zhang, C. Dong, Z. Li, H. Yao, J. Wang and G. Li, *J. Alloys Compd.*, 2018, **750**, 607–616.

20 Z. Khan, B. Senthilkumar, S. Lim, R. Shanker, Y. Kim and H. Ko, *Adv. Mater. Interfaces*, 2017, **4**, 1700059.

21 H. Pang, S. Wang, W. Shao, S. Zhao, B. Yan, X. Li, S. Li, J. Chen and W. Du, *Nanoscale*, 2013, **5**, 5752–5757.

22 K. V. Sankar, S. C. Lee, Y. Seo, C. Ray, S. Liu, A. Kundu and S. C. Jun, *J. Power Sources*, 2018, **373**, 211–219.

23 B. Li, P. Gu, Y. Feng, G. Zhang, K. Huang, H. Xue and H. Pang, *Adv. Funct. Mater.*, 2017, **27**, 1605784.

24 H. Li, H. Yu, J. Zhai, L. Sun, H. Yang and S. Xie, *Mater. Lett.*, 2015, **152**, 25–28.

25 M. C. Liu, J. J. Li, Y. X. Hu, Q. Q. Yang and L. Kang, *Electrochim. Acta*, 2016, **201**, 142–150.